Potential step voltammetry: an approach to corrosion rate measurement of reinforcements in concrete

J.E. Ramón[a,b,1], J.M. Gandía-Romero[a,c,*], R. Bataller[a], M. Alcañiz[a,d], M. Valcuende[c] and J. Soto[a,b].

[a] Interuniversity Research Institute for Molecular Recognition and Technological Development, Universitat Politècnica de València - Universitat de València, Camino de Vera s/n, 46022 Valencia, Spain.
[b] Department of Chemistry, Universitat Politècnica de València, Camino de Vera s/n, 46022 Valencia, Spain.
[c] Department of Architectural Construction, Universitat Politècnica de València, Camino de Vera s/n, 46022 Valencia, Spain.
[d] Department of Electronic Engineering, Universitat Politècnica de València, Camino de Vera s/n, 46022 Valencia, Spain.

* Corresponding author.
E-mail address: joganro@csa.upv.es

ABSTRACT

This paper presents a Potentiostatic Step Voltammetry approach to corrosion rate measurement of reinforcements in concrete. We have termed this approach PSV-TE since it is based on the Tafel extrapolation method, but with the added advantage that long and slow potentiodynamic scans are no longer required to obtain the Tafel slopes. In this way, the irreversible polarization of rebars is prevented, so PSV-TE is considered to be a non-destructive method. The Tafel slopes are obtained by fitting the current-time response of the system to a theoretical model which we have outlined and validated previously. In this way, the concrete's electrical resistance and double layer capacity are also obtained. In this study, the optimal PSV-TE design has been established and validated on a range of reinforced concrete specimens. Results show minimal deviation between PSV-TE and reference methods. Therefore, PSV-TE is part of the corrosion monitoring system we have patented.

KEYWORDS: potential step voltammetry; non-destructive technique; steel corrosion; reinforced concrete; durability.

1. INTRODUCTION

In the 70s, different electrochemical techniques were developed to evaluate corrosion processes in different metal-electrolyte systems [1], including reinforced concrete [2]. These types of techniques analyse the electrochemical response of steel-concrete systems by applying a perturbation that displaces them from their equilibrium state. The parameter usually determined to quantify the process is the corrosion current density, i_{CORR}. For many years, Tafel extrapolation (TE) was considered one of the most accurate methods for determining i_{CORR}. It consists of extrapolating the anodic and cathodic linear regions of the polarization curve to the corrosion potential (E_{CORR}). These linear regions are usually obtained when the electrode potential is moved far away from the E_{CORR} by applying a slow potentiodynamic scan. As a consequence, TE measurements are time consuming and can produce irreversible polarization of the electrode [3]. In practice,

1 Since the work described in the article was done, this author has moved to: Instituto de Ciencias de la Construcción Eduardo Torroja, CSIC, C/Serrano Galvache No.4, Madrid, 28033, Spain.

the most widely used method is Linear Polarization Resistance (LPR), proposed by Stern and Geary [4]. It is based on the linear relationship between current and potential in the vicinity of the E_{CORR}. The polarization resistance (R_P) is determined from the slope of this linear region and enables us to calculate i_{CORR} by using the Stern-Geary equation:

$$i_{CORR} = \frac{B}{A \cdot R_P} \quad (1)$$

where A is the area of the embedded steel in cm^2. The Stern-Geary constant B is obtained from anodic (b_A) and cathodic (b_C) Tafel slopes:

$$B = \frac{b_A \cdot b_C}{2.303 \cdot (b_A + b_C)} \quad (2)$$

In corrosion of steel in concrete, B is assigned a value of 13 or 52 mV for active and passive samples, respectively. In practice, adopting 26 mV as an averaged B value is recommended, since the resulting error of 2 can be considered negligible when determining i_{CORR} in passive reinforcements [5, 6]. Although the potentiodynamic polarization technique is one of the most widely used to perform LPR measurements, there are a number of factors that limit its application for on-site measurements [6, 7]. The most common alternatives are those based on the transient response analysis, which stand out for their speed. On one hand, there are those methods where R_P is determined from the time constant of galvanostatic [8], coulostatic [9], or potentiostatic [10] potential transients. On the other hand, there are those methods where R_P is obtained by curve-fitting analysis of the galvanostatic [11] or potentiostatic [12] transients, although the difficulties in finding an accurate model for steel-concrete systems has limited their implementation in practice [13]. Research carried out to obtain R_P from electrochemical impedance spectroscopy (alternate current) has also been important [14], as have been efforts to find an accurate model for the steel-concrete system using this technique.

In any case, as indicated above, all R_P methods always introduce a certain degree of inaccuracy. This is widely known; however, it has generated some interest in exploring alternatives that allow i_{CORR} to be determined with an accuracy closer to the TE method but without disturbing the system. The first proposed methods consisted of calculating i_{CORR} from the steady-state current of a series of potentiostatic pulses [15] or from a number of points from the polarization curve [16]. However, the equations used involve laborious calculations or are only applicable under very specific conditions [17]. Simpler methods are those based on the graphical analysis of the polarization curve near the E_{CORR} [18] or of a potential transient [19], despite the possible inaccuracies characteristic of any graphical method. To solve this problem, some authors proposed directly fitting the polarization curves to theoretical models [20]. However, the software implemented in this method did not always provide consistent results [21-22]. One of the most interesting proposals consisted of obtaining just the linear regions of the polarization curves needed to apply the TE method [23]. However, these approaches were based on galvanostatic or galvanodynamic techniques, which do not allow us to control the applied polarization level. Consequently, these methods did not go beyond specific laboratory research.

Therefore, there are enough reasons to continue researching corrosion rate techniques. In recent years, the potentiostatic pulse technique has been applied in different areas of interest, such as electronic tongues [24], quality control of water [25], beverages, and food [26]. The advantage of this technique lies in selecting and controlling the polarization applied to the sample. In addition, as we already described in previous papers [27, 28], potential steps can be arranged in symmetrical patterns in order to ensure that no irreversible polarization

takes place on the electrode surface. Therefore, the potentiostatic pulse technique can be repeatedly implemented without damaging the studied system, which is highly advantageous in monitoring routines.

In recent years, authors have been focused on exploring the possibilities of potentiostatic pulse voltammetry to assess the corrosion rate of reinforced concrete. While potentiostatic pulse technique has already been used in studies of steel corrosion in concrete [10, 12], the corrosion rate measurement is primarily based on the LPR method. In this paper we outline an alternative approach with Potentiostatic Step Voltammetry (PSV) in which the corrosion rate is accurately obtained, since it is based on the Tafel extrapolation method (TE). We have termed this method PSV-TE, and its main advantage is that the usual long and slow voltammetry scans are not required to obtain the Tafel slopes, so the corrosion rate determination is faster and possible irreversible polarization of rebars is prevented. In previous works [27, 28] we have outlined and validated both the pulse pattern and the theoretical model on which the PSV-TE is based. This method has been conceived for use in the embeddable corrosion monitoring system for steel reinforced structures which we have patented [29].

2. PRINCIPLES OF THE METHOD

The goal of the proposed PSV-TE approach is to construct each of the linear regions of the polarization curve (anodic and cathodic) through several single points in order to determine the corrosion current using the Tafel extrapolation method, but in a rapid and non-disturbing way. As seen in Fig. 1-a, the abscissa of each of these points corresponds to the applied overpotential (η), which must lay within a range in which the polarization curve shows a linear trend. The value of the ordinate corresponds to the Faradaic current (I_F) that passes through the system for such η.

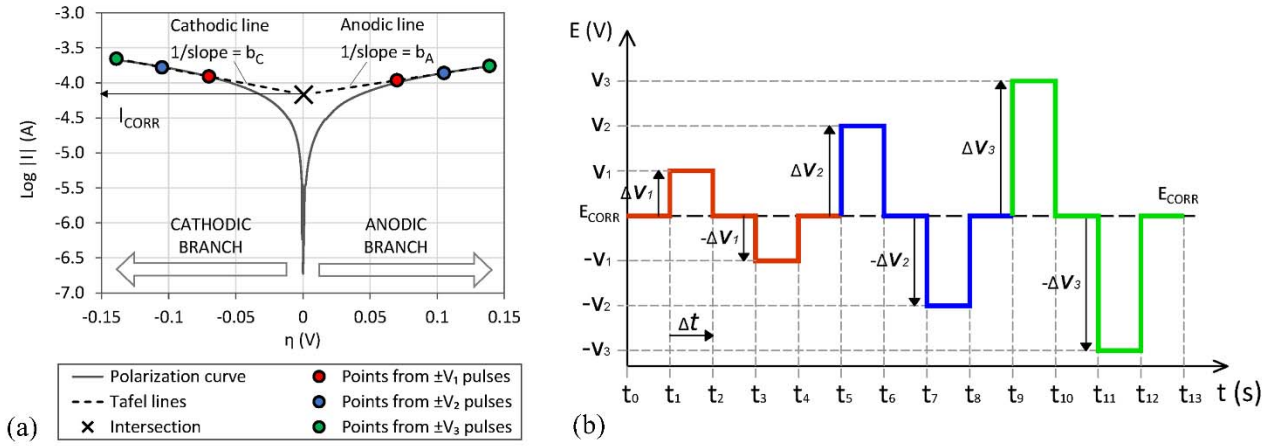

Figure 1. Principles of the proposed PSV-TE approach: (a) representation of a polarization curve together with the I_F-η points obtained by curve-fitting the response to (b) a symmetrical potentiostatic pulse pattern of various amplitudes.

For some authors, I_F corresponds to the steady-state current when applying a potentiostatic pulse [30], which entails applying long pulses that could irreversibly alter the system [13]. An alternative is to use a shorter pulse and fit the resulting experimental curve to an equivalent circuit (CEq) that models the steel-concrete interface [31]. Over the years, different variations of the Randles simple model have been proposed [32]. In our current paper, the model shown in Fig. 2 is adopted, since a close approximation of this circuit has been used previously to model the steel-concrete response when applying a potential step [31]. It will be referred to hereinafter as mixed CEq. This circuit considers the two main general processes involved in corrosion of reinforcement, namely the Faradaic and the non-Faradaic processes. As we already described in a previous

work [27], these two processes should be considered in parallel, so that two well-differentiated branches appear in the proposed circuit. On the one hand, the R_1-[C_1/R_P] branch corresponds to the Faradaic process, where R_1 is the resistance associated with the ionic transport of those species involved in the corrosion reaction given by R_P. The capacitor C_1 represents the capacitive behaviour of the steel-concrete interface in the in the localized corrosion area. On the other hand, the R_2-C_2 branch corresponds to the non-Faradaic process, where R_2 is the ionic resistance of those species (Ca^{+2}, Na^+, K^+, OH^-) not involved in the electron transfer (corrosion reaction) whose capacitive behaviour is given by C_2.

Here we present Eq. (3), first proposed to model the current-time response of the adopted circuit (Fig. 2) when applying a potentiostatic pulse (ΔV). This equation is derived from the generic expression validated in a previous work [27] when the pulse pattern is intended to be in a symmetrical arrangement as shown in Fig. 1-b.

$$I(\Delta V_j; t) = \frac{\Delta V_j}{R_1} e^{-(t-t_j)\frac{R_p+R_1}{R_p R_1 C_1}} + \frac{\Delta V_j}{R_p + R_1} \cdot \left(1 - e^{-(t-t_j)\frac{R_p+R_1}{R_p R_1 C_1}}\right) + \frac{\Delta V_j}{R_2} e^{-\frac{t-t_j}{R_2 C_2}} \quad (3)$$

It is shown as follows how the relevant corrosion parameters are obtained from Eq. (3). To begin with, we apply t = 0 in Eq. (3):

$$I_0 = \Delta V \cdot \left(\frac{1}{R_1} + \frac{1}{R_2}\right) = \frac{\Delta V}{R_S} \quad (4)$$

I_0 is the non-Faradaic current that passes through the mixed CEq (Fig. 2) for t = 0 and it depends on the resistance to the ionic movement through the concrete pore solution (R_1 and R_2), which is usually known as the electrical resistance of the medium (R_S). The value of R_S for the mixed CEq is obtained by applying:

$$\frac{1}{R_S} = \frac{1}{R_1} + \frac{1}{R_2} \quad (5)$$

The Faradaic current that passes through the circuit, once the steady state has been reached, corresponds to I_F, whose value can be determined from Eq. (3) when $t \rightarrow \infty$:

$$I_F = \frac{\Delta V}{R_1 + R_p} \quad (6)$$

In common steel-concrete systems, $R_1 + R_P$ is high enough to assume that the double layer capacity (C_{dl}) of the steel-concrete interface can be estimated from capacitors C_1 and C_2 (Fig. 2) according to:

$$C_{dl} = \frac{C_1 + C_2}{A} \quad (7)$$

where A is the evaluated area of steel in cm^2.

According to Fig. 2, the value of the ohmic drop at steady state corresponds to $I_F \cdot R_1$. Therefore, it is easy to determine the value of the applied overpotential (η):

$$\eta = \Delta V - (I_F \cdot R_1) \quad (8)$$

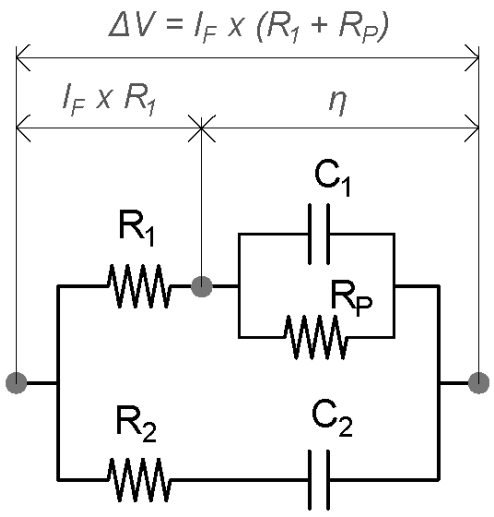

Figure 2. Mixed Equivalent Circuit proposed to model the response of the steel-concrete interface to a potential step. The voltage in steady-state condition is depicted at different parts of the circuit.

The different components of the mixed CEq are determined by fitting Eq. (3) to the experimental I-t curve from a potentiostatic pulse. The fitting procedure consists of minimizing the sum of error squares. I_F and η are obtained by applying Eqs. (6) and (8), respectively.

If three pulses of different amplitudes are applied (ΔV_1, ΔV_2, and ΔV_3 within the linear region of the polarization curve), the three I_F-η points needed to construct the anodic or the cathodic Tafel line are obtained, based on whether +ΔV or -ΔV pulses (Fig. 1) are applied. Therefore, to determine both Tafel lines in a single test, it would be enough to apply a sequence that includes three anodic pulses ($+\Delta V_1$, $+\Delta V_2$ and $+\Delta V_3$) and three cathodic pulses ($-\Delta V_1$, $-\Delta V_2$ and $-\Delta V_3$). Therefore, we propose using the pulse sequence found in Fig. 1-b. This sequence starts from the corrosion potential (E_{CORR}) and alternates anodic and cathodic excitation pulses, applying relaxation steps between them (return to E_{CORR}), that is: $E_{CORR}/+\Delta V_1/E_{CORR}/-\Delta V_1/E_{CORR}/+\Delta V_2/E_{CORR}/-\Delta V_2/E_{CORR}/+\Delta V_3/E_{CORR}/-\Delta V_3/E_{CORR}$. As we have outlined previously [27, 28], this sequence is intended to ensure that the accumulated charge at the end of the test is practically zero and, therefore, that no irreversible polarization of the sample occurs.

Curve-fitting analysis of the excitation pulses of Fig. 1-b gives the six I_F-η points required to construct both Tafel lines (Fig. 1-a), whose slopes b_A and b_C can be applied to Eq. (2) to obtain parameter B. The i_{CORR} value is obtained from the intersection of both lines or from only one of them at η = 0 if the opposite half-reaction is diffusion-controlled. The values of R_S (Eq. (5)), C_{dl} (Eq. (7)), and R_P correspond to the average of the six excitation pulses.

In summary, PSV-TE has been conceived as a non-destructive method to obtain the parameters R_S, R_P, C_{dl}, i_{CORR} and B in a single test without significantly polarizing the studied system. Therefore, PSV-TE is the measurement method employed in the corrosion monitoring system that we have patented for use in reinforced structures [29].

3. EXPERIMENTAL

3.1. Concrete specimens

Twenty-seven cylindrical specimens of dimensions ø50 x 100 mm were manufactured using micro concrete with a water/cement ratio of 0.8. The detailed composition is shown in Table 1.

This dosage, outside the standards limits for structural concrete, was intentionally used in the experimental design in order to achieve a high degree of porosity, which accelerates the diffusion of aggressive agents. It was considered the most efficient way to achieve a significant amount of corrosion mass loss over a reasonable period of time, and then be able to validate the PSV-TE method against the gravimetric method. To study the corrosion processes, a corrugated carbon steel bar of 10 mm in diameter and 100 mm in length was embedded in each of the specimens (Fig. 3). Both ends were sealed with epoxy resin, although one was left partially uncovered in order to connect the wiring needed to apply the tests. The effective working surface of embedded steel in each sample was 18.42 cm^2.

Table 1. Composition of the micro concrete.

Component	kg/m^3
Cement CEM I 42.5R	250
Water	200
Sand (0/4)	1471
Gravel (4/6)	638

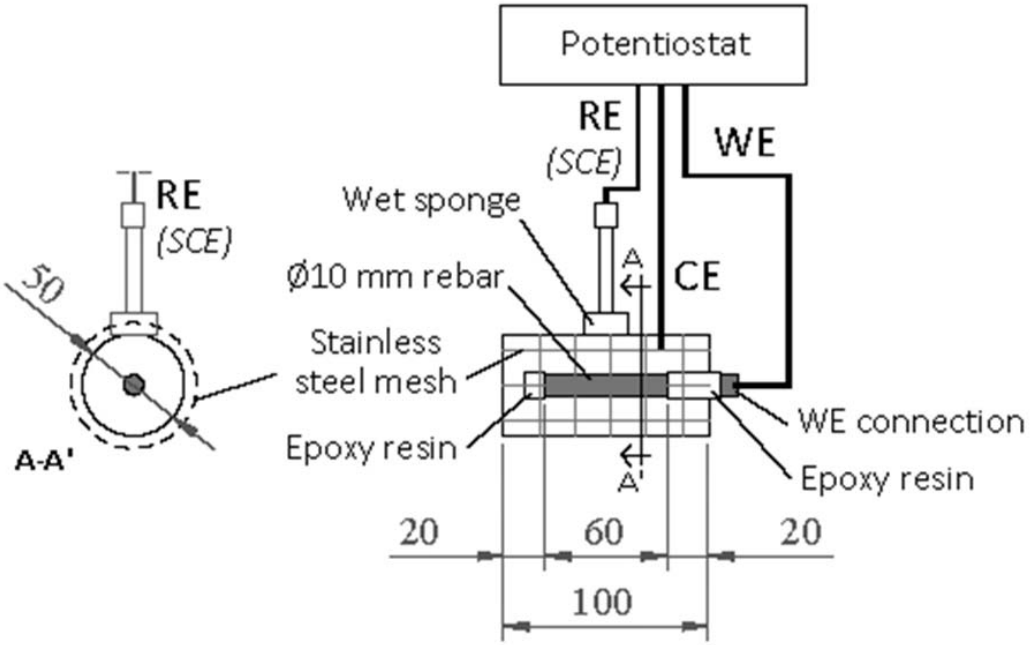

Figure 3. Diagram of the concrete specimen and experimental setup for electrochemical measurements. Dimensions are in mm.

3.2. Laboratory conditions

After 48 hours of casting, all the specimens were demoulded and placed in a curing chamber until they reached the age of 28 days. After this period, the specimens were divided into 3 groups (A, B, and C) of 9 samples each. In order to enhance the steel corrosion, the specimens of group A were subjected to an accelerated carbonation process by exposing the specimens in a carbonation chamber with 3% carbon dioxide at 65% relative humidity. According to the results obtained from the phenolphthalein tests carried out in twinned samples, it took 42 days to carbonate the entire concrete cover, which was 20 mm thick. After this phase, groups A and B were submerged in a 35g/L NaCl solution, while group C was inserted into a saturated solution of $Ca(OH)_2$ (pH ≈ 13). The NaCl solution simulated the concentration of chlorides in seawater and the saturated lime solution kept the concrete in a non-aggressive environment. The specimens were kept under such conditions for 48 months.

3.3. Measurement procedure

Fig. 3 shows the experimental set up used to apply the different electrochemical techniques. It is a three-electrode cell in which the embedded rebar is the working electrode (WE). As a reference electrode (RE), a saturated calomel electrode (SCE) was used. As a counter-electrode (CE), a stainless-steel mesh was mounted externally surrounding the specimen so that the electric field was as homogeneous as possible. Between the concrete surface and the CE, a wet cloth was placed to ensure optimal electrical contact. The equipment used to perform the electrochemical measurements was the Autolab PGSTAT 100. All experiments were carried out inside a Faraday cage at room temperature (20 ± 2°C).

The measurement procedure unfolded as follows:

1. Initially, the electrical resistance between the CE and the WE (R_{COND}) was measured in each specimen by means of the conductivity-meter Knick Portavo-904. These measurements were subsequently used to validate the R_S value determined by PSV-TE.

2. Prior to applying each polarization technique, the corrosion potential (E_{CORR}) of the embedded rebar was determined by measuring the open circuit potential (OCP) versus a SCE placed as shown in Fig. 3. The E_{CORR} to be considered corresponds to the OCP value once stability was reached ($dE/dt \leq 0.03$ mV/s). This measurement was made with the same instrument used to apply the polarization techniques.

3. The first technique applied was cyclic sweep voltammetry (CSV) starting from E_{CORR} and reaching ± 20 mV at a scan rate of 10 mV per minute. The R_P was obtained from the slope of the linear region that appears in the voltammogram once the ohmic drop was compensated for. The i_{CORR} parameter was obtained by applying Eq. (1) with B = 26 mV. This is the Linear Polarization Resistance method of Stern and Geary, hereinafter referred to as LPR. From the distance between the lesser sloping sides of the voltammogram in the E_{CORR} (ΔI_{Ecorr}), the double layer capacity (C_{dl}) was determined as:

$$C_{dl} = \frac{\Delta I_{Ecorr}}{2 \cdot v \cdot A} \tag{9}$$

where v is the scan rate in $V \cdot s^{-1}$ and A is the working area of the embedded rebar in cm^2. This method for obtaining C_{dl} has previously been used by other authors [6] and it will hereinafter be referred to as CSV.

4. Next, the PSV-TE method was applied (Fig. 1). In order to study the optimal design of the pulse pattern initially proposed in Fig. 1-b, different pulse duration (Δt) values in the range from 10 to 120 seconds were tested. The applied potentials $\pm\Delta V_1$, $\pm\Delta V_2$ and $\pm\Delta V_3$ presented in Fig. 1-b correspond to 70, 105 and 140 mV. The i_{CORR} and the rest of the corrosion parameters (R_S, R_P, C_{dl}, and B) were obtained according to the methodology explained in Section 2.

5. Finally, i_{CORR} was determined through Tafel extrapolation of the semilogarithmic representation of the polarization curves (log | I | vs η) obtained by applying the linear sweep voltammetry technique at a scan rate of 10 mV per minute. Initially, an anodic scan was applied from E_{CORR} to E_{CORR} +140 mV. To ensure that the E_{CORR} returned to the values initially recorded (with a difference of ±5 mV), the cathodic sweep from E_{CORR} to E_{CORR} -140 mV was applied after a period of 24 hours. This method will hereinafter be referred to as TE.

The complete measurement procedure was applied once a month for the 48 months of study. However, the PSV-TE and the conductivity-meter measurements were applied weekly. The objective was to obtain a thorough follow-up of i_{CORR} with PSV-TE and thus to be able to accurately calculate the theoretical mass loss by corrosion (Δm) according to:

$$\Delta m = \frac{i_{CORR} \cdot A \cdot t \cdot M}{n \cdot F} \quad (10)$$

where t is the monitored period in seconds, M is the atomic mass of steel (55.1 g/mol), n is equal to 2 (number of electrons released in the oxidation process), and F is the Faraday constant (96485 $C \cdot mol^{-1}$).

At the end of the study, the samples were broken in half by an indirect tensile test (Brazilian test) to determine real Δm and thus validate the PSV-TE measurements. To do so, the gravimetric method was used following the guidelines of the standard ASTM G1-03 [33].

3.4. Statistical parameters

Where calculating the deviation between two parameters was required, one of them being the exact or experimental value (X_i) and the other the predicted or calculated value (P_i), the corresponding Relative Error (ε_r) was determined:

$$\varepsilon_r = \left|\frac{X_i - P_i}{X_i}\right| \cdot 100 \quad (11)$$

Likewise, to determine the deviation between the fitted and the experimental curves, the Mean Absolute Percentage Error (MAPE) was used:

$$MAPE = \frac{\sum_{i=1}^{n} \left|\frac{X_i - P_i}{X_i}\right| \cdot 100}{n} \quad (12)$$

In this case, X_i and P_i correspond to the values of the experimental and fitted curves respectively, while n is the number of points. Another parameter that has been used in the successive sections to compare two data sets is the coefficient of determination R^2 obtained from the regression between X_i and P_i. It should be noted that, in all the statistical parameters described here, P_i is the value of interest we want to analyse by comparison with X_i, the reference value.

4. RESULTS AND DISCUSSION

To facilitate the analysis and discussion of the results, this section has been divided into two phases:

Design of the method: i) Here we demonstrate the validity of the mixed equivalent circuit (CEq) found in Fig. 2 for modelling the steel-concrete systems by applying the PSV-TE technique. After validating this model, ii) we analyse the most efficient design of the potentiostatic pulse sequence to be used in PSV-TE. It is a matter of determining the optimal pulse duration (Δt) and the $\pm\Delta V_1$, $\pm\Delta V_2$ and $\pm\Delta V_3$ values (Fig. 1-a) in order to obtain the Tafel slopes quickly and reliably.

Validation of the method: Here we compare the results of R_S, R_P, C_{dl} and i_{CORR} obtained by PSV-TE to reference methods.

4.1. Design of the method

4.1.1. Equivalent circuit

Of all the specimens, three representative measurements have been selected here: high (sample 1), moderate (sample 2) and low (sample 3). These are three well-differentiated measurements which were selected from all the results achieved over the study (48 months) in accordance with the corrosion level criteria established in the standard UNE 112072 [34]. As a result, the high corrosion sample belongs to group A, the medium corrosion sample belongs to group B and the low corrosion sample belongs to group C.

To check whether the mixed CEq of Fig. 2 adequately models steel-concrete systems, we analysed the correspondence when fitting Eq. (3) to the experimental current-time curves. Taking into account that the objective here is not to determine i_{CORR}, the complete pulse sequence of Fig. 1-b was not analysed, but rather just a single pulse of +70 mV. The pulse duration (Δt) was long enough to reach the quasi-steady state. In other words, the current remained practically constant towards the end of each pulse. For samples 1 and 2 (high and medium corrosion levels) Δt was 120 seconds, whereas for sample 3 (passive state) Δt was 50 seconds.

As shown in Fig. 4, Eq. (3) gives accurate fittings for all corrosion levels. The obtained R^2 value was always higher than 0.98 and the MAPE coefficient presented small values in all cases (< 0.7%). Therefore, the mixed CEq is valid for modelling the response of steel-concrete systems when applying potentiostatic pulses such as those included in the sequence of Fig. 1-b.

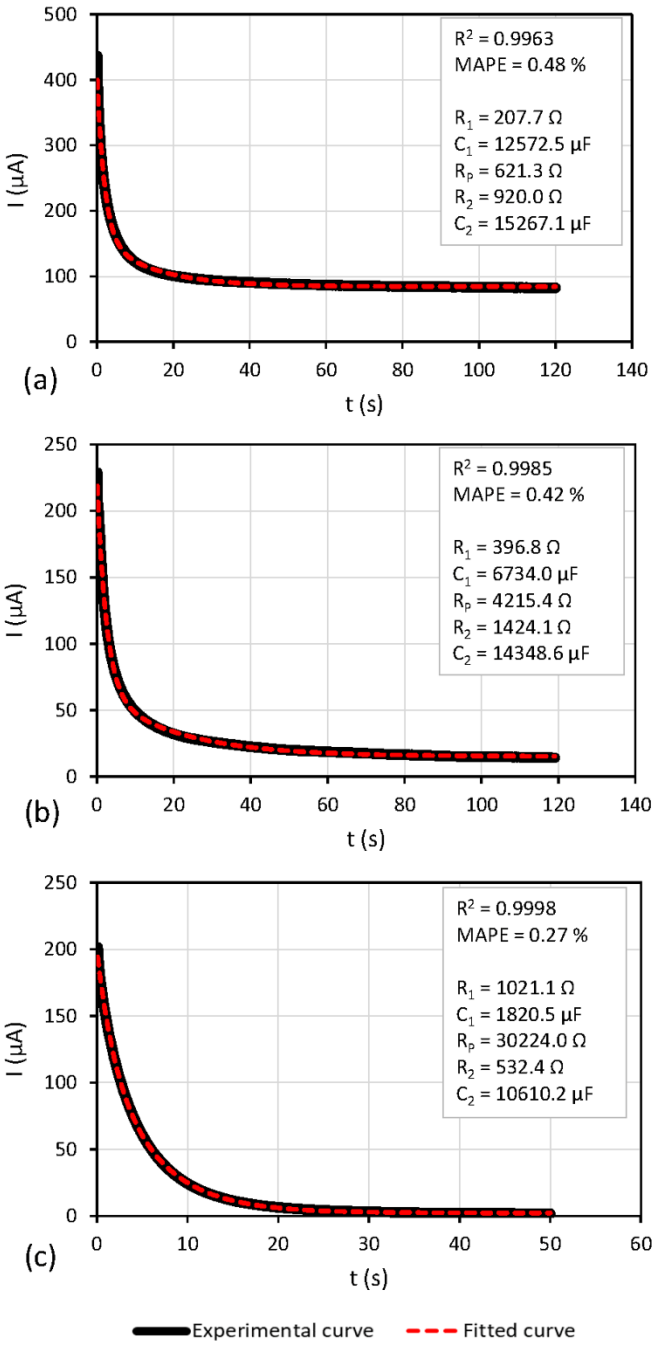

Figure 4. Current-time curve obtained by applying a pulse of ΔV = +70 mV (black line) together with the fitted curve (red dashed line) for the model given by Eq. (3) in three samples with different corrosion levels: high (a), medium (b) and low (c). The curve fitting results are displayed for each sample (inside the box).

4.1.2. Pulse sequence

This section studies the design of the pulse pattern of PSV-TE and its ability to provide high reliability when determining i_{CORR} by using TE as the reference method. To do this, the three samples selected for section 4.1.1 are also analysed here.

The polarization curves obtained with TE for the three specimens over a range of E_{CORR} ±140 mV are shown in Fig. 5 in a semilogarithmic scale. In all cases, these curves present Tafelian behaviour, since both the anodic and the cathodic branches exhibit a linear trend from an overpotential (η) of approximately ±60 mV. Therefore, for the sequence in Fig. 1-b, $\pm\Delta V_1$, $\pm\Delta V_2$ and $\pm\Delta V_3$ must be within the range of 60 to 140 mV, so the following values were selected: ±70, ±105 and ±140 mV. This polarization is high enough to ensure that the linear parts of the polarization curve are obtained. Otherwise, inaccurate results are obtained since Tafel slopes are determined too close to the E_{CORR} at the polarization curve (Fig. 1-a) and, consequently, the corrosion rate value is underestimated. In any case, the polarization must not be much higher than necessary in order to avoid an undesirable excessive polarization of the embedded steel.

Each pulse was applied for the duration (Δt) previously established in Section 4.1.1. An accurate curve fitting of the experimental response was achieved, since MAPE and R^2 coefficients are in the same order as those shown in Fig. 4. As seen in Fig. 6, the Faradaic current (I_F) values obtained from this fitting are very close to the polarization curves.

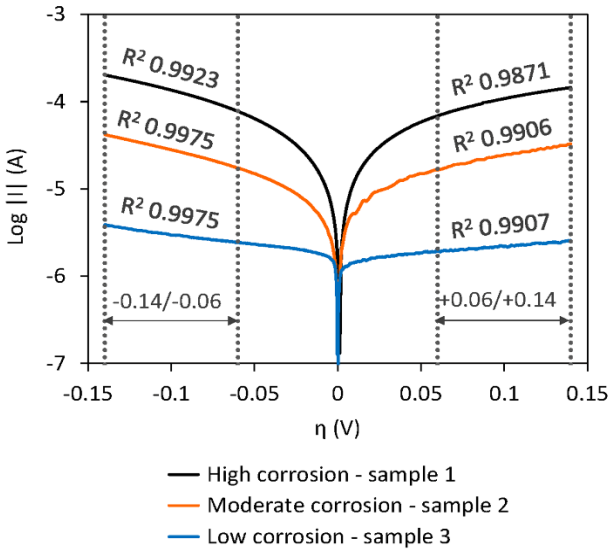

Figure 5. Semilogarithmic plot of the polarization curves of three specimens with different corrosion levels.

As an example, Fig. 7 compares the accumulated charge (Q) in specimen 1 when applying TE and PSV-TE. It shows that a large amount of charge remains accumulated after applying TE. This explains the 24-hour period necessary between cathodic and anodic scans to get the samples back to their equilibrium state (E_{CORR}). This gap could underlie the small deviations observed between both techniques in specimens 2 and 3. On the other hand, the residual charge after applying the PSV-TE was minimal. This fact is reflected in the $|Q_{PSV\text{-}TE}| / |Q_{TE}|$ ratio obtained for sample 1, which was 3.34% and 2.71% with respect to the anodic and the cathodic TE scans. Very similar values were also obtained in samples 2 and 3.

In any case, the i_{CORR} and B values from both methods correspond well (Fig. 6). In addition, the value of these parameters is consistent with the corrosion level of the samples. Parameter B decreases as i_{CORR} increases, which is consistent with the results of prior studies [35]. In all cases, the R^2 coefficient of the Tafel lines, both anodic and cathodic, was equal to or greater than 0.99 for both methods.

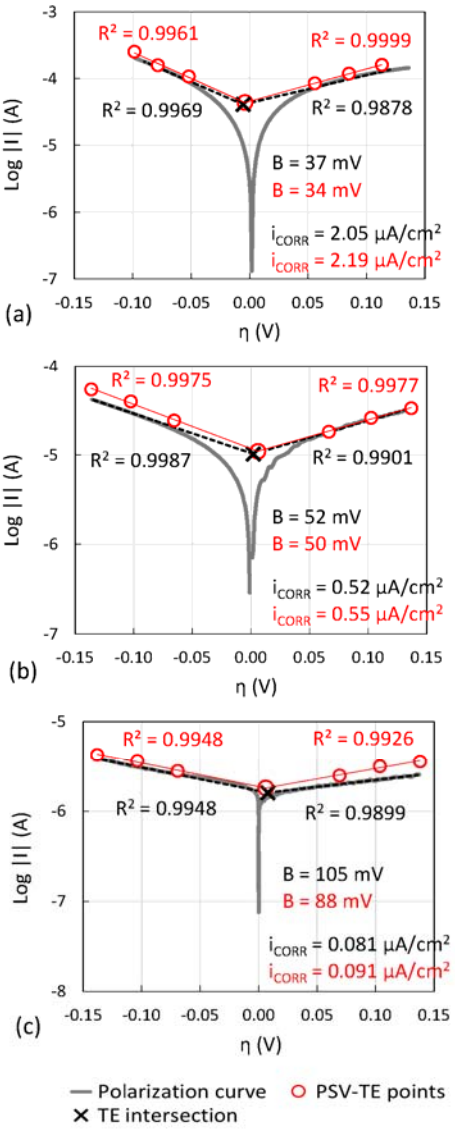

Figure 6. Comparison of the results obtained for samples 1 (a), 2 (b) and 3 (c) with TE (black) and PSV-TE (red).

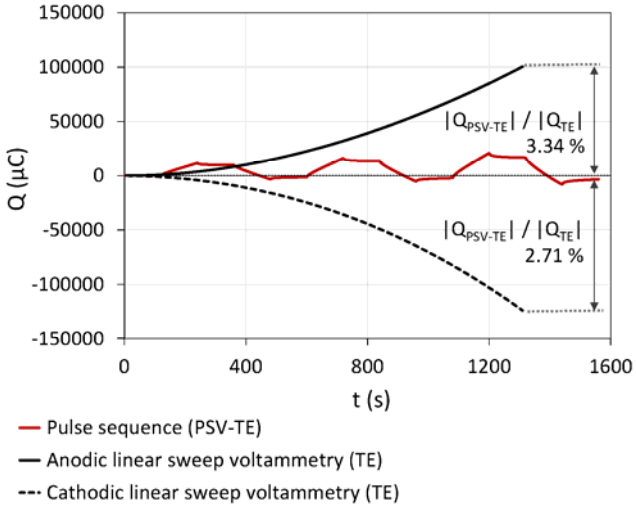

Figure 7. Comparison between the accumulated charge in specimen 1 when applying PSV-TE versus TE (for both anodic and cathodic scans).

For practical reasons, it is convenient to reduce the duration of the pulse pattern when determining i_{CORR}, but ideally it should be done without losing reliability. To determine the optimal pulse duration (Δt), the experimental current-time curves were fitted, progressively reducing the Δt value. As an example, the analysis of the pulse ΔV = +140 mV obtained for specimen 1 is shown in Fig. 8-a. It is clear that as Δt decreases, the quality of the fitting worsens. In fact, the MAPE (Eq. (12)) exceeds 5% for values with Δt less than 30 seconds in specimens 1 and 2 (Fig. 8-b). In the case of specimen 3, the goodness of fit does not substantially worsen until the pulse duration is shorter than 20 seconds.

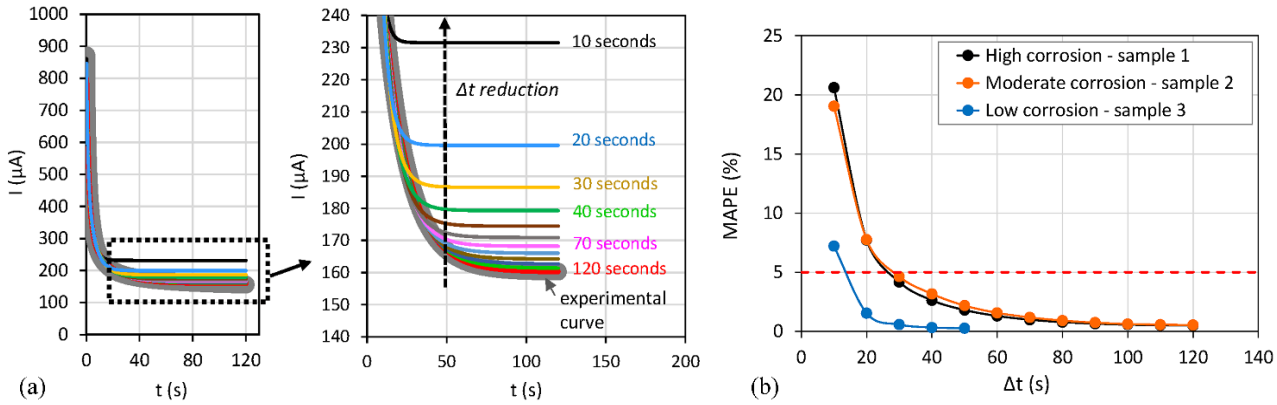

Figure 8. Current-time curve fitting corresponding to the pulse ΔV = +140 mV applied to specimen 1 for different Δt values (a). MAPE values related with the goodness of fit according to the Δt used (b).

Fig. 9 shows the Relative Error (Ɛr) (Eq. (11)) associated with the different corrosion parameters as a function of the Δt used. This error was calculated with respect to the value of the parameter obtained for the maximum Δt. In specimen 1 (high corrosion), C_{dl} is the most affected parameter. In specimen 2 (intermediate corrosion), a similar variation is observed in all the parameters (with the exception of R_S). In specimen 3 (passive state), i_{CORR} is strongly altered up to values of Ɛr over 100% for the shortest duration.

It should be noted that, as the Δt is shortened, the transient response of the steel-concrete interface moves further away from the quasi-steady state, which is the hypothetical ideal condition we should consider to reliably determine the corrosion parameters, and which can be found at a pulse duration of 50 seconds. Fig. 9 shows that as the pulse duration (Δt) is shortened, the Relative Error (Ɛr) with respect to the longest duration increases. This increase is magnified as the corrosion level decreases, which means that approaching the steady-state (by using potentiostatic pulses with the maximum Δt possible) is highly necessary in order to obtain reliable results in passive specimens. This behaviour may be due to the fact that the amount of experimental data gathered with the instrument is reduced as the pulse duration is shortened. This could be considered an additional error source, especially when the current response measured is too low (passive specimens) and, consequently, the reduced amount of experimental points could present certain dispersion, which could lead to unreliable results when carrying out the curve fitting analysis by using the model from Fig. 2. This could explain the strong increase in Relative Error (Ɛr) observed for the low corrosion specimen in Fig. 9-c.

Nonetheless, in general, the Ɛr value exceeds 25% when Δt is less than or equal to 40 seconds. Taking into account this reasonable limit, the Δt value used in the pulse pattern of Fig. 1-b is set at 50 seconds regardless of whether the rebar is in active or passive state.

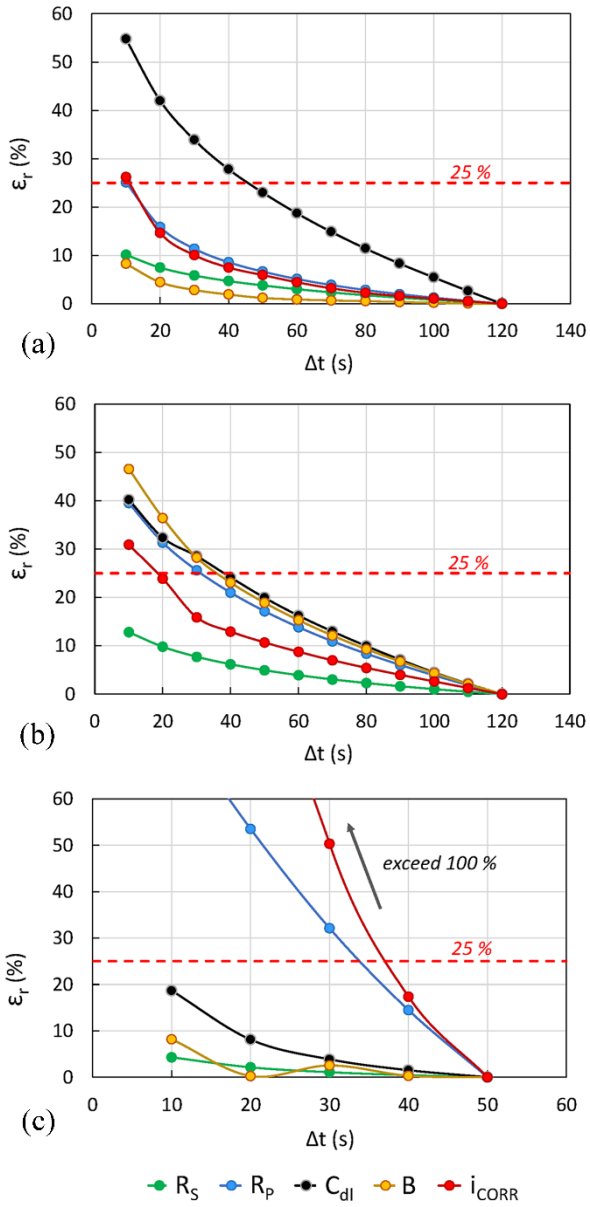

Figure 9. Relative error (Ɛr) for the different corrosion parameters as a function of the Δt used in the pulse pattern. Results for specimens 1 (a), 2 (b), and 3 (c) are shown.

4.2. Method validation

In this section, we validate the capability of the proposed PSV-TE approach to determine the different corrosion parameters in embedded rebars. For this purpose, we analyse the results of the set of 27 concrete specimens exposed to environments of different aggressiveness.

As stated above (see Section 4.1.2), the pulse pattern (Fig. 1-b) has a duration (Δt) of 50 seconds per pulse, and the applied potentials (±ΔV) correspond to 70, 105 and 140 mV. Although the samples were tested periodically during the 48 months of the study, only results for three specific ages (16, 32 and 48 months) are presented here in order to facilitate the analysis.

4.2.1. Polarization resistance and corrosion density

Fig. 10-a shows the correlation between the R_P values obtained by PSV-TE and LPR. Both methods correspond well (R^2 = 0.9265), with slightly lower values observed for PSV-TE with respect to LPR (< 2% according to the slope of the regression line). Fig. 10-b shows good correlation obtained when comparing i_{CORR} from PSV-TE versus TE. Although the R^2 coefficient is very similar to that obtained in the LPR versus TE regression (Fig. 10-c), the deviation of the regression in Fig. 10-b is lower. In particular, PSV-TE tends to overestimate i_{CORR} by about 3% with respect to TE, whereas LPR tends to underestimate i_{CORR} by about 22%.

The LPR deviation may be due to the fact that the B coefficient used in Eq. (1) was set at 26 mV for all cases. Fig. 11 shows the experimental value of B obtained from TE and PSV-TE for each group of samples. As usual in these cases, the samples in the passive state (group C) present the highest values. In general, it is observed that the B values from TE are higher than those determined by PSV-TE. These differences are magnified in group C (passive state), where TE presents considerable dispersion. In any case, the obtained values do not seem too far from those outlined in the literature [36]. Using the experimental value of B in i_{CORR} calculations did not lead to an improvement in the LPR versus TE regression, but rather the opposite (Fig. 10-d). Therefore, as other authors have previously argued [35], it is difficult to establish an accurate correlation between parameter B and i_{CORR}.

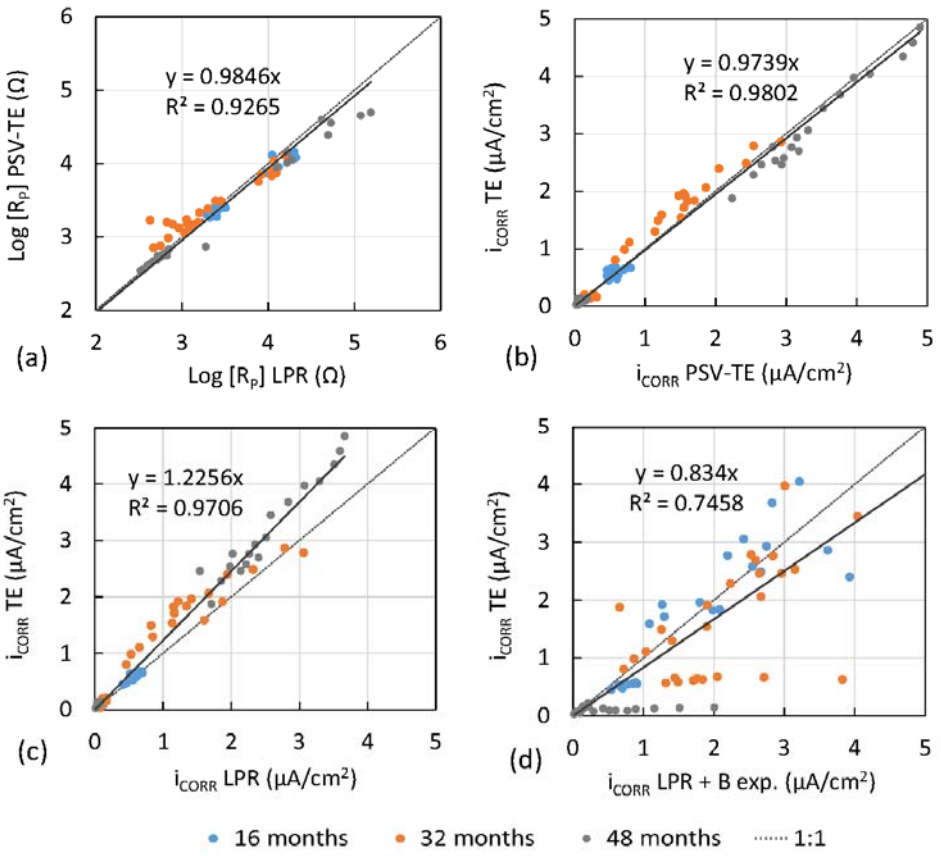

Figure 10. Logarithmic regression of the R_P value obtained by PSV-TE and LPR (a), and linear regression between the i_{CORR} value obtained using TE versus PSV-TE (b), TE versus LPR (c) and TE versus LPR + experimental B (d).

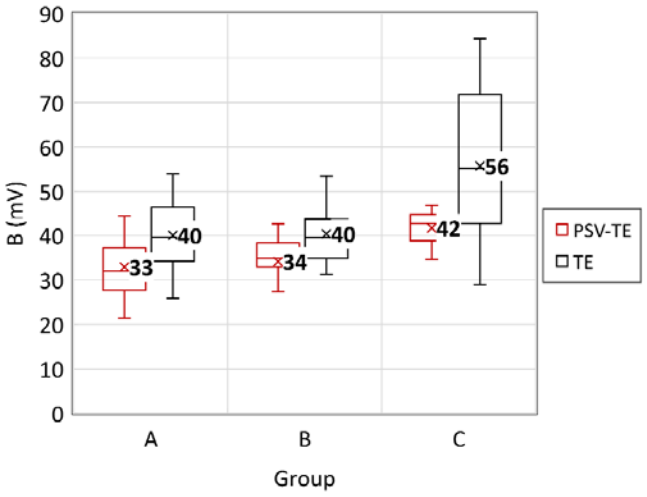

Figure 11. Box plot where the values of the B coefficient obtained by means of TE and PSV-TE are compared.

Moreover, Fig. 12 compares the mass loss (Δm) calculated from the PSV-TE i_{CORR} measurements for the 48-month follow-up, and the real mass loss determined by the gravimetric method at the end of the study. The R^2 coefficient is 0.9635, which indicates a good linear correlation between both methods. The slope of the regression line is 0.9097, which indicates a slight overestimation (≈ 9%) of the Δm by PSV-TE.

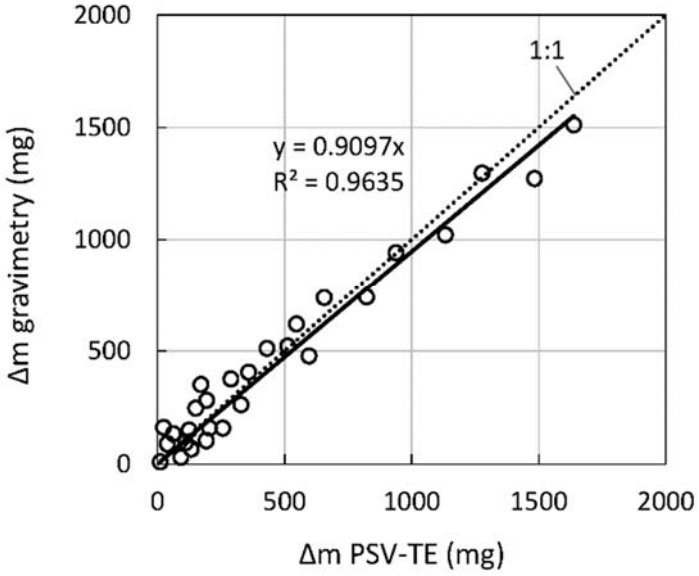

Figure 12. Regression between the mass loss of steel due to corrosion (Δm) obtained by the gravimetric method and the PSV-TE method for all concrete specimens at the end of the study.

4.2.2. Double layer capacity

A good agreement between the C_{dl} values determined by PSV-TE and CSV was obtained (R^2 = 0.9527), as shown in Fig. 13-a. The values obtained by PSV-TE are approximately 27% higher. In general, an increase in the C_{dl} value is observed as the corrosion level increases. This phenomenon could be related to the accumulation of corrosion products at the steel-concrete interface that behave as electrolytic capacitors. In fact, if C_{dl} is plotted versus i_{CORR} (Fig. 13-b), a certain direct linear relationship is observed (R^2 = 0.8667).

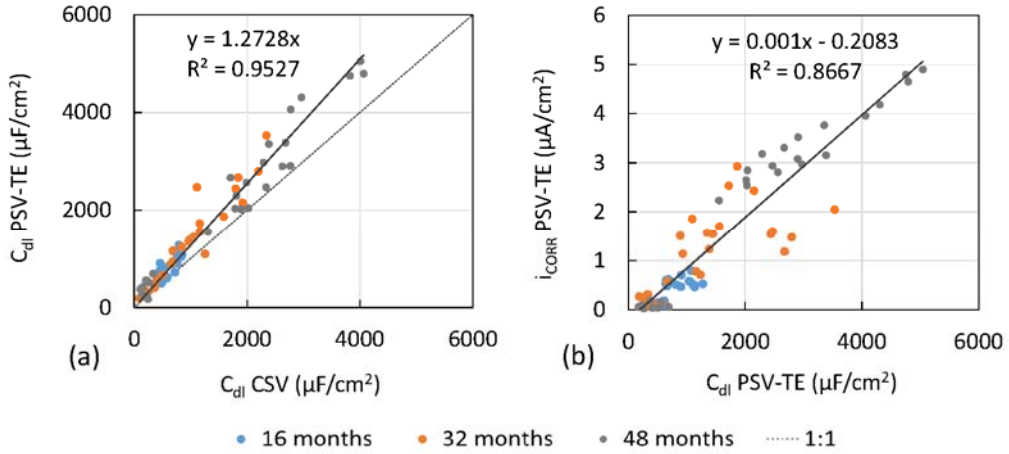

Figure 13. Regression between the C_{dl} values obtained by CSV and PSV-TE (a) and regression between i_{CORR} and C_{dl} determined by PSV-TE (b).

4.2.3. Electrical resistance of the medium

Fig. 14 shows the correlation between the R_S parameter obtained by PSV-TE and the electrical resistance measured by the conductivity-meter (R_{COND}) for the 27 specimens. In order to ensure a homogeneous distribution of results, the values presented here do not correspond exclusively to the values at 16, 32 and 48 months, but to shorter time intervals.

It should be noted that R_S and R_{COND} are not totally equivalent. The R_S parameter corresponds to the electrical resistance between the RE and the WE (according to the model in Fig. 2), while R_{COND} was determined by applying alternate current between the CE and the WE. In this case, the distances of the RE and the CE with respect to the WE were similar (Fig. 3), which makes $R_{S\text{-}CE/WE} \approx R_{S\text{-}RE/WE}$, and therefore $R_{COND} \approx R_S$. In fact, good agreement between both parameters is observed ($R^2 = 0.9748$), with the values obtained by PSV-TE being approximately 10% higher (Fig. 14).

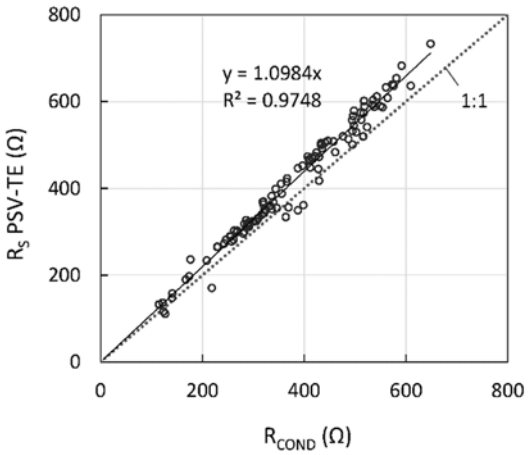

Figure 14. Regression between the electrical resistance measured with the conductivity-meter (R_{COND}) and the R_S values obtained by PSV-TE.

4.2.4. Precision of the method

Once the accuracy of PSV-TE was validated (see Sections 4.2.1, 4.2.2 and 4.2.3), its precision was also verified. To this end, three samples from each group were tested at the end of the study by all three

electrochemical methods: LPR, TE and PSV-TE. To determine the precision of these methods, each of the samples was measured five times within a short time interval (10 days), and the corresponding coefficient of variation (CV) was then calculated. Fig. 15 shows the CV value for each of the corrosion parameters in relation to the group of samples and the method used.

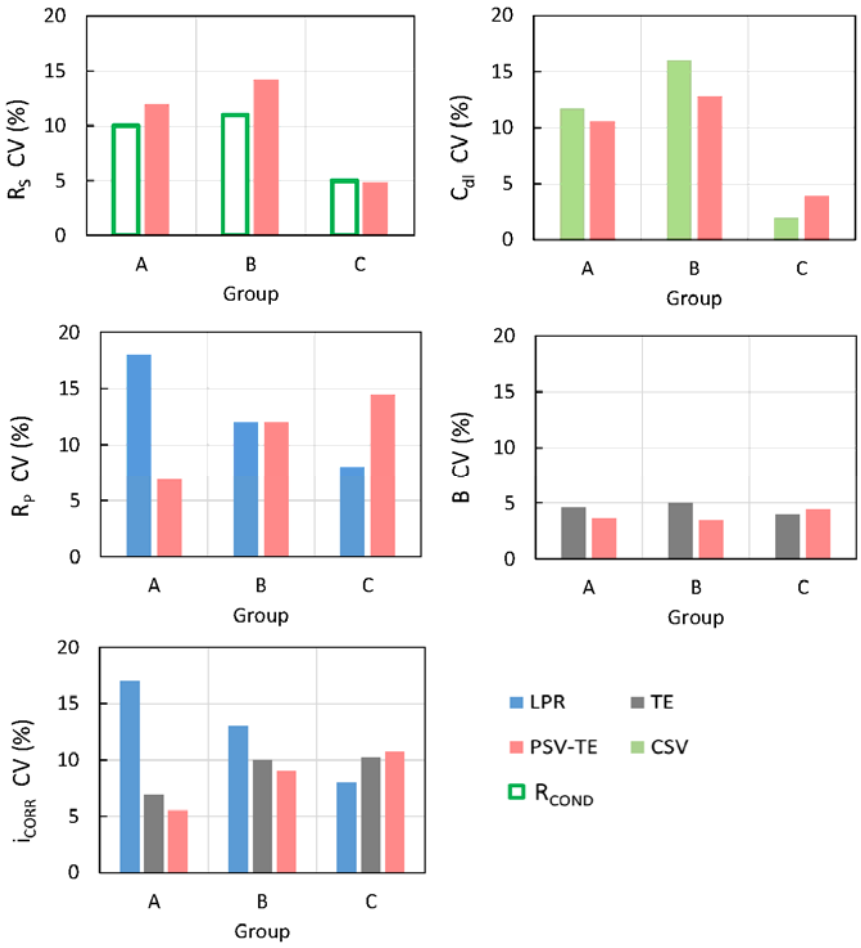

Figure 15. Values of the coefficient of variation (CV) of the different corrosion parameters obtained by applying LPR, CSV, TE, and PSV-TE five consecutive times on three samples of each group (A, B and C).

As for the electrical resistance (R_S), PSV-TE has CV values very similar to those obtained with the conductivity-meter (R_{COND}). For group C, in passive state, the precision of both methods is very similar. When determining the R_P, some differences are observed between LPR and PSV-TE. The CV is smaller in LPR as the corrosion level decreases (group C). This phenomenon could be related to the shape of the voltammogram (Fig. 16). When the sample is in active state, the linear section where R_P is determined is not easily observed. On the contrary, when the sample is in passive state, the linear zone is perfectly defined. With PSV-TE, the greater variability of R_P appears in the passive specimens. This could be related to the very low current intensities recorded in these samples at the end of the pulses (quasi-steady state), which compromises the sensitivity of the electronic device employed.

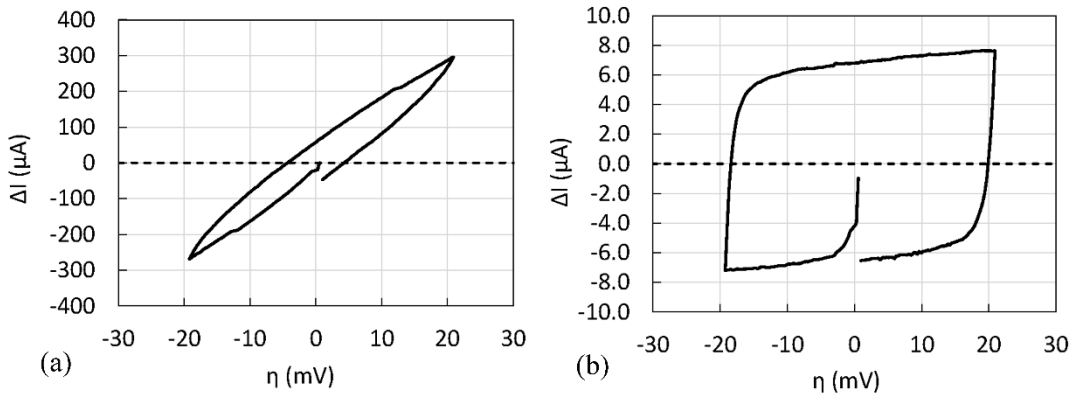

Figure 16. Polarization curves obtained by cyclic sweep voltammetry in samples of group A (a) and group C (b) respectively.

There are no significant differences between PSV-TE and CSV when determining C_{dl}. In this case, the CV reaches its minimum value in group C. In the case of CSV, this effect could again be related to the shape of the polarization curve. As seen in Fig. 16-b, the voltammogram for the passive samples takes the form of a clearly defined parallelogram and, consequently, the distance between the lesser sloping sides (required to calculate C_{dl}) is easy to determine.

As for the i_{CORR} parameter, certain differences between all the different methods are observed. Specifically, in the active samples (groups A and B) the precision of PSV-TE is greater than that of the other methods. The differences with LPR are magnified especially in group A, where the specimens are more corroded. In fact, this trend was previously observed in the R_P parameter. In comparison, the differences between PSV-TE and TE are much smaller, with CV values of the three methods being very similar in the passive specimens (group C). With regard to the B coefficient, PSV-TE is slightly more precise in groups A and B, mirroring the TE method in group C.

In general, the precision of PSV-TE does not differ significantly from that of the other reference methods. In fact, CV values higher than 15% have not been obtained in any case.

5. CONCLUSIONS

We have proposed a Pulse Step Voltammetry approach (PSV-TE) for corrosion rate measurement of reinforcements in concrete. It is based on the Tafel extrapolation method, but performed by fitting the potentiostatic pulse response to a theoretical model. From the experimental validation of PSV-TE, the following conclusions have been drawn:

The electrical resistance (R_S), the polarization resistance (R_P), and the double layer capacity (C_{dl}) of the steel-concrete interface are obtained by fitting the PSV-TE curves to a modified Randles circuit which we have described and validated in previous works [27, 28].

PSV-TE is based on the well-known Tafel extrapolation method for calculating the corrosion current density (i_{CORR}), but Tafel slopes are obtained more quickly than with the original method and, consequently, without risk of producing the irreversible polarization of rebars. This is achieved by applying a pattern that alternates anodic and cathodic pulses of E_{CORR} ±70, ±105 and ±140 mV,

interposing relaxation steps (return to E_{CORR}) between them. A pulse duration of 50 seconds can be used, for both active and passive embedded rebars.

As compared to reference methods, PSV-TE tends to slightly overestimate the corrosion rate. This deviation is around 3% with respect to the classical Tafel extrapolation method, and close to 10% with respect to the gravimetric method. The precision of PSV-TE to determine R_S, R_P and C_{dl} is somewhat higher in the samples in active state and similar in the samples in passive state.

In general, the results presented here indicate that PSV-TE is a non-destructive method which can be used successfully to determine the corrosion rate of steel in concrete in addition to other relevant parameters such as R_S, R_P, C_{dl}, and Tafel slopes. In this regard, PSV-TE could be an interesting tool to implement in corrosion monitoring routines of reinforced concrete structures.

DECLARATION OF COMPETING INTEREST

None.

ACKNOWLEDGEMENTS

This work was supported by a pre-doctoral scholarship granted to Jose Enrique Ramon Zamora by the Spanish Ministry of Science and Innovation [grant number FPU13/00911]. We would also like to acknowledge financial support from the Spanish Ministry of Economy and Competitiveness through the national program of oriented research, development and innovation to societal challenges [project number BIA2016-78460-C3-3-R]. The research activity reported in this paper has been performed in the framework of the ReSHEALience project which has received funding from the European Union's Horizon 2020 research and innovation program [number 760824]. We extend our appreciation to Rafa Calabuig and Jesús Martinez, Material Laboratory technicians of the ETSIE of the Universitat Politècnica de València, for their invaluable cooperation in the experimental work.

REFERENCES

[1] F. Mansfeld, The Polarization Resistance Technique for Measuring Corrosion Currents, Advances in Corrosion Science and Technology, 6 (1976) 163–262. https://doi.org/10.1007/978-1-4684-8986-6_3.

[2] C. Andrade, J.A. González, Quantitative measurements of corrosion rate of reinforcing steels embedded in concrete using polarization resistance measurements, Mater. Corros., 29-8 (1978) 515–519.

[3] Z. T. Chang, B. Cherry, M. Marosszeky, Polarisation behaviour of steel bar samples in concrete in seawater. Part 1: Experimental measurement of polarisation curves of steel in concrete, Corros. Sci. 50 (2008) 357–364. https://doi.org/10.1016/j.corsci.2007.08.009.

[4] M. Stern, A.L. Geary, Electrochemical Polarization. I. A Theoretical Analysis of the Shape of Polarization Curves, J. Electrochem. Soc. 104 (1957) 56–63. https://doi.org/10.1149/1.2428496.

[5] J.A. González, J. Albéniz, S. Feliu, Valores de la constante B del método de resistencia de polarización para veinte sistemas metal-medio diferentes, Rev. Metal. 32 (1996) 10–17. https://doi.org/10.3989/revmetalm.1996.v32.i1.926.

[6] J.A. González, A. Molina, M. L. Escudero, C. Andrade, Errors in the electrochemical evaluation of very small corrosion rates-I. Polarization resistance method applied to corrosion of steel in concrete, Corros. Sci. 25 (1985) 917–930. https://doi.org/10.1016/0010-938X(85)90021-6.

[7] J.R. Scully, Polarization resistance method for determination of instantaneous corrision rates, Corrosion 56 (2000) 199–218. https://doi.org/10.5006/1.3280536.

[8] S. Feliu, J.A. González, M.C. Andrade, Confinement of the electrical signal for in situ measurement of polarization resistance in reinforced concrete, Materials Journal 87 (1990) 457-460. https://doi.org/10.14359/1830.

[9] K. Kanno, M. Suzuki, Y. Sato, Coulostatic Method for Rapid Estimation of Corrosion Rate; Water to SB46 in 1N H2SO4 and SS41 in Distilled, Boshoku Gijutsu 26 (1977) 697–701. https://doi.org/10.3323/jcorr1974.26.12_697.

[10] D.M. Bastidas, J.A. González, S. Feliu, A. Cobo, J.M. Miranda, A quantitative study of concrete-embedded steel corrosion using potentiostatic pulses, Corrosion 63 (2007) 1094–1100. https://doi.org/10.5006/1.3278327.

[11] B. Elsener, O. Klinghoffer, T. Frolund, E. Rislund, Y. Schiegg, H. Bohni, Assessment of Reinforcement Corrosion by Means of Galvanostatic Pulse Technique, Proceeding of the International Conference on Repair of Concrete Structures, in A. Blankvoll (Ed.), Svolvaer, Norway, Norwegian Public Roads Administration, 1997, pp. 391–400.

[12] G.K. Glass, C.L. Page, N.R. Short, J.Z. Zhang, The analysis of potentiostatic transients applied to the corrosion of steel in concrete, Corros. Sci. 39 (1997) 1657–1663. https://doi.org/10.1016/S0010-938X(97)00071-1.

[13] V. Feliu, J.A. González, S. Feliu, Corrosion estimates from the transient response to a potential step, Corros. Sci. 49 (2007) 3241–3255. https://doi.org/10.1016/j.corsci.2007.03.004.

[14] C. Andrade, L. Soler, C. Alonso, X.R. Nóvoa, M. Keddam, The importance of geometrical considerations in the measurement of steel corrosion in concrete by means of AC impedance, Corr. Sci., 37 (1995) 2013-2023. https://doi.org/10.1016/0010-938X(95)00095-2.

[15] S. Barnartt, Two-point and three-point methods for the investigation of electrode reaction mechanisms, Electrochim. Acta 15 (1970) 1313–1324. https://doi.org/10.1016/0013-4686(70)80051-2.

[16] R. Bandy, The Simultaneous Determination of Tafel Constants and Corrosion Rate - A New Method, Corros. Sci. 20 (1980) 1017–1028. https://doi.org/10.1016/0010-938X(80)90081-5.

[17] V.S. Beleevskii, K.A. Konev, V.V. Novosadov, V.Y. Vasil'ev, Estimating corrosion current and tafel constants from the curvature of voltammetric curves near the free-corrosion potential, Prot. Met. 40 (2004) 566–569. https://doi.org/10.1023/B:PROM.0000049521.65336.25.

[18] K.B. Oldham, F. Mansfeld, Corrosion rates from polarization curves: A new method, Corros. Sci. 13 (1973) 813–819. https://doi.org/10.1016/S0010-938X(73)80021-6.

[19] K. Kanno, M. Suzuki, Y. Sato, Tafel slope determination of corrosion reaction by the coulostatic method, Corros. Sci. 20 (1980) 1059–1066. https://doi.org/10.1016/0010-938X(80)90084-0.

[20] F. Mansfeld, Tafel Slopes and Corrosion Rates from Polarization Resistance Measurements, Corrosion 29 (1973) 397–402. https://doi.org/10.5006/0010-9312-29.10.397.

[21] G. Rocchini, The determination of tafel slopes by the successive approximation method, Corros. Sci. 37 (1995) 987–1003. https://doi.org/10.1016/0010-938X(95)00009-9.

[22] F. Mansfeld, Tafel slopes and corrosion rates obtained in the pre-Tafel region of polarization curves, Corros. Sci. 47 (2005) 3178–3186. https://doi.org/10.1016/j.corsci.2005.04.012.

[23] V. Lakshminarayanan, S.R. Rajagopalan, Applications of exponential relaxation methods for corrosion studies and corrosion rate measurement, Proc. Indian Acad. Sci. 97 (1986) 465–477. https://doi.org/10.1007/BF02849206.

[24] I. Campos, M. Alcañiz, R. Masot, J. Soto, R. Martínez-Máñez, J-L. Vivancos, L. Gil, A method of pulse array design for voltammetric electronic tongues, Sensors Actuators, B Chem. 161 (2012) 556–563. https://doi.org/10.1016/j.snb.2011.10.075.

[25] M.C. Martínez-Bisbal, E. Loeff, E. Olivas, N. Carbó, F.J. García-Castillo, J. López-Carrero, I. Tormos, F.J. Tejadillos, J.G. Berlanga, R. Martínez-Máñez, M. Alcañiz, J. Soto, A voltammetric electronic tongue for the quantitative analysis of quality parameters in wastewater, Electroanalysis 29 (2017) 1147–1153. https://doi.org/10.1002/elan.201600717.

[26] L. Sobrino-Gregorio, R. Bataller, J. Soto, M.I. Escriche, Monitoring honey adulteration with sugar syrups using an automatic pulse voltammetric electronic tongue, Food Control 91 (2018) 254-260. https://doi.org/10.1016/j.foodcont.2018.04.003.

[27] J.E. Ramón, A. Martínez-Ibernón, J.M. Gandía-Romero, R. Fraile, R. Bataller, M. Alcañiz, E. García-Breijo, J. Soto, Characterization of electrochemical systems using potential step voltammetry. Part I: Modeling by means of equivalent circuits, Electrochim. Acta 323 (2019) 134702. https://doi.org/10.1016/j.electacta.2019.134702.

[28] A. Martínez-Ibernón, J.E. Ramón, J.M. Gandía-Romero, I. Gasch, M. Valcuende, M. Alcañiz, J. Soto, Characterization of electrochemical systems using potential step voltammetry. Part II: Modeling of reversible systems, Electrochim. Acta 328 (2019) 135111. https://doi.org/10.1016/j.electacta.2019.135111.

[29] M. Alcañiz, R. Bataller, J.M. Gandía-Romero, J.E. Ramón, J. Soto, M. Valcuende, Sensor, red de sensores, método y programa informático para determinar la corrosión en una estructura de hormigón armado, invention patent No. ES2545669, Publication date 19 de January 2016.

[30] P. Rodriguez, E. Ramirez, J. Gonzalez, Methods for studying corrosion in reinforced concrete, Mag. Concr. Res. 46 (1994) 81–90. https://doi.org/10.1680/macr.1994.46.167.81.

[31] S. Feliu, J.A. Gonzalez, C. Andrade, V. Feliu, The determination of the corrosion rate of steel in concrete by a non-stationary method, Corros. Sci. 26 (1986) 961–970. https://doi.org/10.1016/0010-938X(86)90086-7.

[32] V. Feliu, J.A. González, C. Andrade, S. Feliu, Equivalent circuit for modelling the steel-concrete interface. I. Experimental evidence and theoretical predictions, Corros. Sci. 40 (1998) 975–993. https://doi.org/10.1016/S0010-938X(98)00036-5.

[33] ASTM International. G1-03(2017)e1 Standard Practice for Preparing, Cleaning, and Evaluating Corrosion Test Specimens. West Conshohocken, PA; ASTM International, 2017. https://doi.org/10.1520/G0001-03R17E01.

[34] UNE 112072:2011 Spanish Standard. Laboratory measurement of corrosion speed using the polarization resistance technique, 2011.

[35] G. Song, Theoretical analysis of the measurement of polarisation resistance in reinforced concrete, Cem. Concr. Compos. 22 (2000) 407–415. https://doi.org/10.1016/S0958-9465(00)00040-8.

[36] C. Andrade, V. Castelo, C. Alonso, J.A. González, The Determination of the Corrosion Rate of Steel Embedded in Concrete by the Polarization Resistance and AC Impedance Methods, in Corrosion Effect of Stray Currents and the Techniques for Evaluating Corrosion of Rebars in Concrete, edited by Chaker, V. (West Conshohocken, PA: ASTM International, 1986), 43-63. https://doi.org/10.1520/STP18302S.

FIGURE CAPTIONS

Figure 1. Principles of the proposed PSV-TE approach: (b) representation of a polarization curve along with the I_F-η points obtained by curve fitting the response to (a) a symmetrical potentiostatic pulse pattern of various amplitudes.

Figure 2. Mixed Equivalent Circuit proposed to model the response of the steel-concrete interface to a potential step. The voltage in steady-state condition is depicted at different parts of the circuit.

Figure 3. Scheme the concrete specimen and experimental set up for electrochemical measurements. Dimensions are in mm.

Figure 4. Current-time curve obtained by applying a pulse of ΔV = +70 mV (black line) together with the fitted curve (red dashed line) for the model given by Eq. (3) in three samples with different corrosion levels: high (a), medium (b) and low (c). The curve fitting results are displayed for each case (inside the box).

Figure 5. Semilogarithmic plot of the polarization curves of three specimens with different corrosion levels.

Figure 6. Comparison of the results obtained for samples 1 (a), 2 (b) and 3 (c) with TE (black) and PSV-TE (red).

Figure 7. Comparison between the accumulated charge in specimen 1 when applying the pulse sequence technique of PSV-TE and when applying TE (anodic and cathodic).

Figure 8. Current-time curve fitting corresponding to the pulse ΔV = +140 mV applied to specimen 1 for different Δt values (a). MAPE values related with the goodness of fit according to the Δt used (b).

Figure 9. Relative error (Ɛr) for the different corrosion parameters as a function of the Δt used in the pulse pattern. Results for specimens 1 (a), 2 (b), and 3 (c) are shown.

Figure 10. Logarithmic regression of the R_P value obtained by PSV-TE and LPR (a), and linear regression between the i_{CORR} value obtained by TE – LPR (b), TE – LPR + experimental B (c) and TE – PSV-TE (d).

Figure 11. Box plot where the values of the B coefficient obtained by means of TE and PSV-TE are compared.

Figure 12. Regression between the mass loss of steel due to corrosion (Δm) obtained by the gravimetric method and the PSV-TE method for all concrete specimens at the end of the study.

Figure 13. Regression between the C_{dl} values obtained by CSV and PSV-TE (a) and regression between i_{CORR} and C_{dl} determined by PSV-TE (b).

Figure 14. Regression between the electrical resistance measured with the conductivity-meter (R_{COND}) and the R_S values obtained by PSV-TE.

Figure 15. Values of the coefficient of variation (CV) of the different corrosion parameters obtained by applying LPR, CSV, TE, and PSV-TE five consecutive times on three samples of each group (A, B and C).

Figure 16. Polarization curves obtained by cyclic sweep voltammetry in samples of group A (a) and group C (b) respectively.